A New Layered Inorganic−Organic Hybrid Manganese(II) Phosphite: $(C_2H_{10}N_2)[Mn_3(HPO_3)_4]$. Hydrothermal Synthesis, Crystal Structure, and Spectroscopic and Magnetic Properties

Sergio Fernández, José L. Mesa, José L. Pizarro,† Luis Lezama, María I. Arriortua,† Roger Olazcuaga,‡ and Teófilo Rojo*

Departamento de Química Inorgánica and Departamento de Mineralogía-Petrología, Facultad de Ciencias, Universidad del País Vasco, Apdo. 644, E-48080 Bilbao, Spain, and Institut de Chimie de la Matière Condensée de Bordeaux, 33608 Pessac, France

Received February 25, 2000. Revised Manuscript Received April 6, 2000

A new manganese(II) phosphite templated by ethylenediamine has been prepared by hydrothermal synthesis and characterized by X-ray diffraction data and spectroscopic techniques. A study of the evolution of the synthetic process suggests the presence of a manganese(II) phosphite as intermediate in the first steps of the reaction. The $(C_2H_{10}N_2)$-$[Mn_3(HPO_3)_4]$ compound crystallizes in the triclinic space group P-1 with $a = 5.459(1)$ Å, $b = 5.460(2)$ Å, $c = 14.194(5)$ Å, $\alpha = 80.65(2)°$, $\beta = 85.41(1)°$, $\gamma = 60.04(2)°$, $V = 361.7(2)$ Å^3, and $Z = 1$. The compound exhibits a layered structure along the c axis with the ethylenediammonium cations located between the sheets. Within the layers the face-sharing MnO_6 octahedra give rise to trimeric entities which are interconnected by HPO_3 tetrahedra. Studies of luminescence and diffuse reflectance spectroscopies have been carried out. The values of the Dq = 875 cm^{-1} and Racah parameters, $B = 660$ and $C = 3160$ cm^{-1}, have been calculated. The ESR spectra at different temperatures show isotropic signals with a g value of 2.01, which remains unchanged with variation in temperature. The thermal evolution of both the intensity and the line width of the ESR signals shows an increase from room temperature to 4.2 K. From the magnetic measurements the presence of antiferromagnetic interactions in the compound can be observed. The high-temperature magnetic data have been fitted to a model for linear isolated trimers of Mn(II) with a J exchange parameter of −17 K. At temperatures lower than ca. 80 K a long magnetic order, propagated via phosphite anions along the sheets, is established.

Introduction

The synthesis and applications of porous materials are one area of solid-state chemistry that has shown remarkable growth over the past years.[1] Meso- and microporous materials are of great interest from the industrial and academic point of view due to their catalytic, adsorbent, and ion-exchange properties.[2−5] Hydrothermal synthesis is a core in the synthesis of these solids.[6] Understanding of the fundamental processes involved in the synthetic method, especially if templating agents are involved, is sparse. However, it has been shown that the incorporation of hydrogen-bonded organic molecules, such as diammonium cations, via hydrothermal synthesis is a very general method for the attainment of a large variety of novel inorganic−organic hybrid materials such as phosphates, phosphonates, and oxides with a large variety of transition-metal ions.[7−13]

Although to design phases similar to aluminosilicate zeolitic structures has been the subject of main interest to study these materials, the discovery of new compounds with novel structural features has also assumed an important role.[1,14,15] Among the open-framework materials, metal phosphates occupy a first position. A number of works dealing with organically templated

* To whom correspondence should be addressed. E-mail: qiproapt@lg.ehu.es.
† Departamento de Mineralogía-Petrología.
‡ Institut de Chimie de la Matière Condensée de Bordeaux.

(1) Cheetham, A. K.; Ferey, G.; Loiseau, T. *Angew. Chem., Int. Ed. Engl.* **1999**, *38*, 3268.
(2) Clearfield, A. *Chem. Mater.* **1998**, *10*, 2801.
(3) Davis, M. E.; Lobo, R. F. *Chem. Mater.* **1992**, *4*, 756.
(4) Breck, D. W. *Zeolite molecule sieves: structure, chemistry and use*; JohnWiley & Sons: New York, 1974.
(5) Venuto, P. B. *Microporous Mater.* **1994**, *2*, 297.
(6) Barrer, R. M. *Hydrothermal chemistry of zeolites*; Academic Press: London, 1982.
(7) Haushalter, R.; Mundi, L. *Chem. Mater.* **1992**, *4*, 31.
(8) Soghomonian, V.; Chen, Q.; Haushalter, R.; Zubieta, J. *Chem. Mater.* **1993**, *5*, 1690.
(9) Kahn, M.; Lee, Y.; O'Connor, C.; Haushalter, R.; Zubieta, J. *J. Am. Chem. Soc.* **1994**, *116*, 4525.
(10) Zapf, P.; Rose, D.; Haushalter, R.; Zubieta, J. *J. Solid State Chem.* **1996**, *125*, 182.
(11) BeBord, J.; Haushalter, R.; Zubieta, J. *J. Solid State Chem.* **1996**, *125*, 270.
(12) Dhingra, S.; Haushalter, R. *J. Chem. Soc., Chem. Commun.* **1993**, *21*, 1665.
(13) Zhang, Y.; O'Connor, C.; Clearfield, A.; Haushalter, R. *Chem. Mater.* **1996**, *8*, 595.
(14) Choudhury, A.; Natarajan, S.; Rao, C. N. R. *J. Solid State Chem.* **1999**, *146*, 538.
(15) Cavellec, M. R.; Riou, D.; Ferey, G. *Inorg. Chim. Acta* **1999**, *291*, 317.

10.1021/cm001026s CCC: $19.00
Published on Web 07/07/2000

iron phosphates have evidenced a rich structural chemistry in this system.[16−19] In this way, some iron(III) and mixed valence (Fe^{2+}/Fe^{3+}) iron phosphates with three-dimensional, layered structures or isolated single chains are known.[16−22] In some cases, the magnetic and spectroscopic properties of these phases have also been studied.[18,21] Open-framework cobalt(II) phosphates have also been synthesized and studied.[11,23] Recently, an antiferromagnet layered manganese(II) phosphate templated by ethylenediamine has been prepared, and its properties have been reported.[24]

Phosphite, $(HPO_3)^{2-}$, represents a member of the phosphorus oxoanions, which may also be considered as the simplest example of the phosphonate class, $(RPO_3)^{2-}$ with R = H. The structural chemistry of phosphite with elements of the first transition series reveals complex two-dimensional and three-dimensional phases.[25−27] The use of the piperazinium cation as structure-directing agent in the vanadium phosphite system has led to two novel vanadium(IV) phosphites.[28] To determine the role of the template agents in the structure and the physical properties of the metal phosphite compounds, we decided to investigate the manganese(II) phosphite system, exploiting the templating influence of diammonium cations. In this work we report on the hydrothermal synthesis, crystal structure and spectroscopic and magnetic properties of a manganese(II) phosphite templated by ethylenediamine, $(C_2H_{10}N_2)[Mn_3(HPO_3)_4]$. As far as we are aware, this compound is the first inorganic−organic hybrid manganese(II) phosphite.

Experimental Section

Synthesis and Characterization. $(C_2H_{10}N_2)[Mn_3(HPO_3)_4]$ was prepared from reaction mixtures of H_3PO_3 (3.75 mmol), $MnCl_2{\cdot}4H_2O$ (0.75 mmol), and ethylenediamine (4.50 mmol) in a volume of approximately 30 mL of water. The initial pH of the reaction mixture was approximately 7. The synthesis was carried out in a poly(tetrafluoroethylene)-lined stainless steel container under autogenous pressure, filled to approximately 75% volume capacity, and all reactants were stirred briefly before being heated. The reaction mixture was heated at 170 °C for 5 days, followed by slow cooling to room temperature. The final pH of the reaction did not show any significant variation from that measured at the beginning of the reaction. The resulting product was filtered off, washed with ether, and dried in air. Well-formed single crystals with light pink color appeared. The metal ion and phosphorus contents were confirmed by inductively coupled plasma atomic emission spectroscopy (ICP-AES) analysis. C, H, N elemental analysis was also carried out. Found: Mn, 29.9; P, 22.4; C, 4.2; H, 2.4; N, 5.0. $(C_2H_{10}N_2)[Mn_3(HPO_3)_4]$ requires Mn, 30.1; P, 22.7; C, 4.4; H, 2.6; N, 5.1. The density was measured by flotation in a mixture of $CHCl_3/CHBr_3$. The obtained value is 2.5(1) $g{\cdot}m^{-3}$.

Table 1. Crystal Data, Details of Data Collection, and Structure Refinement for the $(C_2H_{10}N_2)[Mn_3(HPO_3)_4]$ Phosphite

empirical formula	$C_2H_{14}N_2O_{12}P_4Mn_3$
molecular weight	546.8
cryst syst	triclinic
space group	*P*-1 (no. 2)
a, Å	5.459(1)
b, Å	5.460(2)
c, Å	14.194(5)
α, deg	80.65(2)
β, deg	85.41(1)
γ, deg	60.04(2)
V, Å^3	361.7(2)
Z	1
ρ_{calcd}, g cm^{-3}	2.511
F(000)	271
T, K	293
radiation, *λ*(Mo Kα), Å	0.710 73
μ (Mo Kα), mm^{-1}	3.086
limiting indices	$-7 < h < 7$, $-7 < k < 7$, $0 < l < 19$
R [$I > 2\sigma(I)$]	R1 = 0.029, wR2 = 0.071[a]
R [all data]	R1 = 0.034, wR2 = 0.074[a]
goodness of fit	1.041

[a] $R1 = [\sum(|F_o| - |F_c|)]/\sum|F_o|$; $wR2 = [\sum[w(|F_o|^2 - |F_c|^2)^2]/\sum[w(|F_o|^2)^2]^{1/2}$; $w = 1/[\sigma^2|F_o|^2 + (xp)^2 + yp]$, where $p = [|F_o|^2 + 2|F_c|^2]/3$, $x = 0.0345$, and $y = 0.6$.

The decomposition curve of $(C_2H_{10}N_2)[Mn_3(HPO_3)_4]$ obtained from the thermogravimetric study reveals a weight loss (ca. 10.5%) between 345 and 420 °C that might be assigned to the thermal decomposition of the ethylenediammonium cation (ca. 11.3% of the total mass). Between ca. 500 and 800 °C additional weight losses were not observed in the thermogravimetric curve. The X-ray diffraction pattern of the residue obtained from the thermogravimetric analysis at 800 °C shows the presence of $Mn_2P_2O_7$. The thermal behavior of $(C_2H_{10}N_2)[Mn_3(HPO_3)_4]$ has also been studied by using time-resolved X-ray thermodiffractometry. The results show that the compound is stable up to ca. 340 °C and the intensity of the monitored (001) peak remains practically unchanged. At around 390 °C a strong decrease of the (001) peak intensity takes place (ca. 44% of the initial intensity), initiating the decomposition of the compound, in good agreement with the thermogravimetric data. Between ca. 555 and 600 °C peaks belonging to the $Mn_2P_2O_7$ pyrophospate appear in the X-ray patterns, which indicates the oxidation of the phosphite compound.

Single-Crystal X-ray Diffraction. A prismatic single crystal of $(C_2H_{10}N_2)[Mn_3(HPO_3)_4]$ with dimensions 0.20 × 0.10 × 0.10 mm was carefully selected under a polarizing microscope and mounted on a glass fiber. Diffraction data were collected at room temperature on an Enraf-Nonius CAD4 automated diffractometer using graphite-monochromated Mo Kα. Details of the crystal data, intensity collection and some features of the structure refinement are reported in Table 1. Lattice constants were obtained by a least-squares refinement of the setting angles of 25 reflections in the range $5° < \theta < 15°$. Intensities and angular positions of two standard reflections were measured every hour and showed no decrease nor misalignment during data collection.

A total of 2173 reflections were measured in the range $2.91° \le \theta \le 29.94°$. A total of 2093 were independent applying the criterion $I > 2\sigma(I)$. Correction for Lorentz and polarization effects was done and also for absorption with the empirical *ψ*

(16) Lii, K.-H.; Huang, Y.-F.; Zima, V.; Huang, C.-Y.; Lin, H.-M.; Jiang, Y.-C.; Liao, F.-L.; Wang, S.-L. *Chem. Mater.* **1998**, *10*, 2599.
(17) Cavellec, M.; Riou, D.; Greneche, J. M.; Ferey, G. *Inorg. Chem.* **1997**, *36*, 2181.
(18) DeBord, J. R. D.; Reiff, W. M.; Warren, C. J.; Haushalter, R.; Zubieta, J. *Chem. Mater.* **1997**, *9*, 1994.
(19) Lii, K. H.; Huang, Y. F. *J. Chem. Soc., Chem. Commun.* **1997**, 1311.
(20) Zima, V.; Lii, K.-H.; Nguyen, N.; Ducouret, A. *Chem. Mater.* **1998**, *10*, 1914.
(21) DeBord, J.; Reiff, W.; Haushalter, R.; Zubieta, J. *J. Solid State Chem.* **1996**, *125*, 186.
(22) Lii, K.-H.; Huang, Y.-F. *J. Chem. Soc., Dalton Trans.* **1997**, 2221.
(23) Chen, J.; Jones, R. H.; Natarajan, S.; Hursthouse, M. B.; Thomas J. M. *Angew. Chem., Int. Ed. Engl.* **1994**, *33*, 639.
(24) Escobal, J.; Pizarro, J. L.; Mesa, J. L.; Lezama, L.; Olazcuaga, R.; Arriortua, M. I.; Rojo, T. *Chem. Mater.* **2000**, *12*, 376.
(25) Sapiña, F.; Gomez, P.; Marcos, M. D.; Amoros, P.; Ibañez, R.; Beltran, D. *Eur. J. Solid State Inorg. Chem.* **1989**, *26*, 603.
(26) Marcos, M. D.; Amoros, P.; Beltran, A.; Martinez, R.; Attfield, J. P. *Chem. Mater.* **1993**, *5*, 121.
(27) Attfield, M. P.; Morris, R. E.; Cheetham, A. K. *Acta Crystallogr.* **1994**, *C50*, 981.
(28) Bonavia, G.; DeBord, J.; Haushalter, R. C.; Rose, D.; Zubieta, J. *Chem. Mater.* **1995**, *7*, 1995.

Table 2. Fractional Atomic Coordinates and Equivalent Isotropic Thermal Parameters ($Å^2 \times 10^3$) for $(C_2H_{10}N_2)[Mn_3(HPO_3)_4]$ (Esd in Parentheses)

atom	*x/a*	*y/b*	*z/c*	U_{eq}[a]
Mn(1)	0.0	0.0	0.0	9(1)
Mn(2)	0.0016(1)	−0.0906(1)	0.2141(1)	10(1)
P(1)	0.6656(1)	0.5550(1)	0.2678(1)	9(1)
P(2)	0.3335(1)	0.3019(1)	0.0746(1)	9(1)
O(1)	0.1716(3)	0.1393(3)	0.1035(1)	12(1)
O(2)	−0.1491(3)	−0.3392(3)	0.3011(1)	14(1)
O(3)	0.3622(3)	0.7230(3)	0.3023(1)	14(1)
O(4)	0.1828(3)	−0.3980(3)	0.1033(1)	12(1)
O(5)	0.7878(3)	−0.7650(3)	0.3008(1)	14(1)
O(6)	−0.3542(3)	0.1280(3)	0.1033(1)	12(1)
N(1)	0.3344(4)	0.1758(4)	0.3798(1)	14(1)
C(1)	0.3629(5)	0.1345(5)	0.4845(2)	21(1)

[a] $U_{eq} = (1/3)\sum_i\sum_j U_{ij}a^*_i a^*_j a_i a_j$.

scan method[29] by using the XRAYACS program.[30] Direct methods (SHELXS 97)[31] were employed to solve the structure. The metal ions and the phosphorus atoms were first located. The oxygen, nitrogen, and carbon atoms were found in difference Fourier maps. The Mn(1) ion occupies a special position with an occupancy factor of 0.5. The structure was refined by the full-matrix least-squares method based on F^2, using the SHELXL 97 computer program.[32] The scattering factors were taken from ref 33. All non-hydrogen atoms were assigned anisotropic thermal parameters. The coordinates of the hydrogen atoms of the phosphite anion were obtained from difference Fourier maps, and those of the ethylenediammonium cation were geometrically placed. The final *R* factors were R1 = 0.029 and wR2 = 0.071. Maximum and minimum peaks in final difference synthesis were 1.338 and −0.770 e $Å^{-3}$. The structure factor parameters have been deposited at the Cambridge Crystallographic Data Centre (CCDC 140146). All drawings were made using the ATOMS program.[34] Fractional atomic coordinates and equivalent isotropic thermal parameters are shown in Table 2. Selected bond distances are given in Table 3.

Physicochemical Characterization Techniques. C, H, N elemental analysis was carried out with a Perkin-Elmer model 240 automatic analyzer. Thermogravimetric measurements were performed in a Perkin-Elmer system 7 DSC−TGA instrument. Crucibles containing approximately 20 mg of sample were heated at 5 °C·min^{-1} under oxygen atmosphere in the temperature range 30−800 °C. X-ray powder patterns were recordered with a PHILIPS X'PERT automatic diffractometer. Cu Kα radiation was employed with steps of 0.02° in 2θ and fixed-time counting of 1 s in the 5° ≤ 2θ ≤ 70° range. Thermodiffractometric experiments were carried out using a PHILIPS X'PERT automatic diffractometer equipped with a variable-temperature stage (Paar Physica TCU2000) with a Pt sample holder. The powder patterns were recorded in 2θ steps of 0.02° in the range 4° ≤ 2θ ≤ 60°, counting for 1 s per step. The measurement time was 50 min per diffractogram (recorded at constant temperature). The temperature was increased at 5 °C·min^{-1} starting from room temperature up to 600 °C. IR spectra (KBr pellets) were obtained with a Nicolet FT-IR 740 spectrophotometer in the 400−4000 cm^{-1} range. Raman spectra were recordered in the 200−3000 cm^{-1} range, with a Nicolet 950FT spectrophotometer equipped with a neodymium laser emitting at 1064 nm. Luminescence measurements were carried out in a Spectrofluorometer Fluorolog-2 SPEX 1680, model F212I, at 6.0 K. The excitation source was a high-pressure xenon lamp emitting between 200 and 1200 nm. The diffuse reflectance spectrum was registered at room temperature on a Cary 2415 spectrometer in the 210−2000 nm range. A Bruker ESP 300 spectrometer was used to record the ESR polycrystalline spectra from room temperature to 4.2 K. The temperature was stabilized by an Oxford Instrument (ITC 4) regulator. The magnetic field was measured with a Bruker BNM 200 gaussmeter, and the frequency inside the cavity was determined using a Hewlett-Packard 5352B microwave frequency counter. Magnetic measurements of powdered samples were performed in the temperature range 4.2−300 K, using a Quantum Design MPMS-7 SQUID magnetometer. The magnetic field was approximately 0.1 T, a value in the range of linear dependence of magnetization vs magnetic field even at 4.2 K.

Table 3. Selected Bond Distances (Å) for $(C_2H_{10}N_2)[Mn_3(HPO_3)_4]$ (Esd in Parentheses)[a]

$Mn(1)O_6$ octahedron		$Mn(2)O_6$ octahedron	
Mn(1)−O(1)/O(1)^{i}	2.216(2)	Mn(2)−O(1)	2.278(2)
Mn(1)−O(4)/O(4)^{i}	2.214(1)	Mn(2)−O(2)	2.110(2)
Mn(1)−O(6)/O(6)^{i}	2.215(1)	Mn(2)−O(4)	2.285(2)
		Mn(2)−O(6)	2.288(2)
		Mn(2)−O(3)^{ii}	2.111(2)
		Mn(2)−O(5)^{iii}	2.108(2)
Mn(1)−Mn(2)	2.999(1)		
$HP(1)O_3$ tetrahedron		$HP(2)O_3$ tetrahedron	
P(1)−O(3)	1.524(1)	P(2)−O(1)	1.531(2)
P(1)−O(2)^{iv}	1.526(2)	P(2)−O(6)^{vi}	1.531(1)
P(1)−O(5)^{v}	1.529(2)	P(2)−O(4)^{v}	1.531(2)
H(1)−P(1)	1.29(3)	H(2)−P(2)	1.26(3)
	$(H_3N(CH_2)_2NH_3)^{2+}$		
N(1)−C(1)	1.475(3)	C(1)−C(1)^{vii}	1.514(3)

[a] Symmetry codes: i = −*x*, −*y*, −*z*, ii = *x*, *y* − 1, *z*, iii = *x* − 1, *y* + 1, *z*, iv = *x* + 1, *y* + 1, *z*, v = *x*, *y* + 1, *z*, vi = *x*+ 1, *y*, *z*, vii = −*x* + 1, −*y*, −*z* + 1.

Results and Discussion

Evolution of the Synthetic Process. To obtain information about the process that takes place in the synthesis of $(C_2H_{10}N_2)[Mn_3(HPO_3)_4]$, a deep study following the reaction times and pH values has been carried out. Different experiments were performed starting from the same experimental conditions as those previously described. In every case the reaction time was 4, 8, 12, 16, 20, 24, 48, 72, 96, and 120 h, the temperature being maintained constant at ca. 170 °C. The pH values measured at the end of each reaction were ca. 7 in all cases. The study of the final products from X-ray powder diffraction measurements (Figure 1a) revealed some interesting data for both the process of formation and the growth of single crystals of $(C_2H_{10}N_2)[Mn_3(HPO_3)_4]$. (i) The X-ray powder diffraction pattern of the mixture of reactives (0 h of reaction time) shows the presence of a product with a low degree of crystalline character. (ii) For reaction times equal to or smaller than ca. 8 h, the $(C_2H_{10}N_2)[Mn_3(HPO_3)_4]$ phase is not yet obtained and the X-ray powder diffraction patterns indicate the existence of an unkown phase. (iii) At reaction times of 12, 16, and 20 h, the $(C_2H_{10}N_2)$-$[Mn_3(HPO_3)_4]$ compound can be obtained as a crystalline phase, but an unknown crystalline compound detected after 4 and 8 h of reaction time also appears. (iv) After ca. 24 h of hydrothermal reaction, very small single crystals of $(C_2H_{10}N_2)$ $[Mn_3(HPO_3)_4]$ were obtained as a unique product. (v) The experiments performed with reaction times between 24 and 120 h indicate that ca. 5

(29) North, A. C. T.; Philips, D. C.; Mathews, F. S. *Acta Crystallogr.* **1968**, *A24*, 351.
(30) Chandrasekaran, A. *XRAYACS: Program for single-crystal X-ray data corrections*; Chemistry Department, University of Massachusetts, Amherst, 1998.
(31) Sheldrick, G. M. *SHELXS 97: Program for the solution of crystal structures*; University of Göttingen, Germany, 1997.
(32) Sheldrick, G. M. *SHELXL 97: Program for the refinement of crystal structures*; University of Göttingen, Germany, 1997.
(33) *International tables for X-ray crystallography*; Kynoch Press: Birmingham, England, 1974; Vol. IV, p 99.
(34) Dowty, E. *ATOMS: A computer program for displaying atomic structures*; Shape Software, 521 Hidden Valley Rd., Kingsport, TN, 1993.

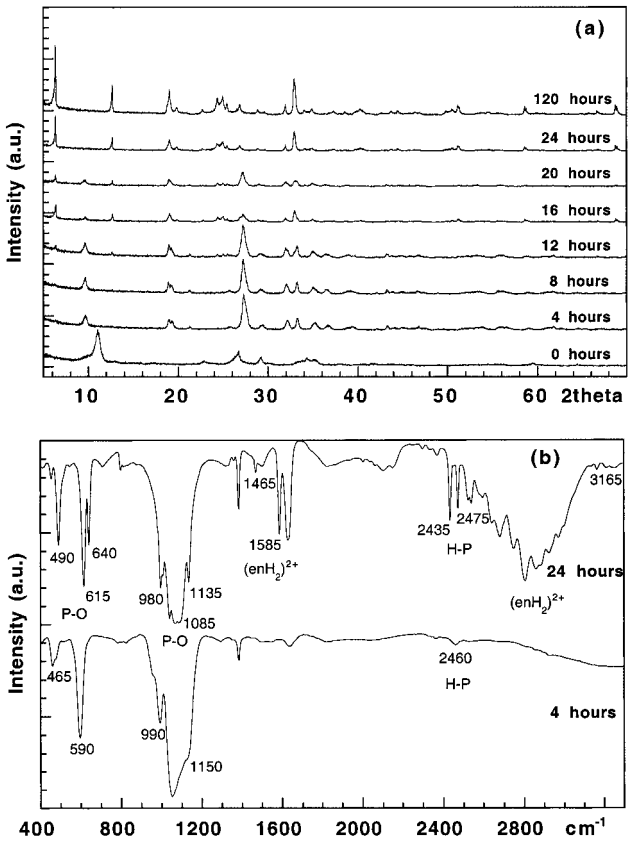

Figure 1. (a) X-ray powder diffraction patterns and (b) IR spectra of the products obtained after several reaction times.

days were necessary to grow suitable single crystals for the X-ray diffraction study.

The IR spectrum of $(C_2H_{10}N_2)[Mn_3(HPO_3)_4]$ obtained after ca. 24 h of reaction time shows the characteristic bands of the phosphite anions and the ethylenediammonium cation [ν(H−P), 2475, 2435 cm^{-1}; $\nu(PO_3)$, 1135, 1085, 980 cm^{-1}; $\nu(PO_3)$, 640, 615, 490, 460 cm^{-1}; $\nu(NH_3^+)$, 3165 cm^{-1}; ν(−CH_2−), 3000−2600 cm^{-1}; δ(−CH_2−), 1515−1465 cm^{-1}; $\delta(NH_3^+)$, 1585 cm^{-1}] (Figure 1b). The IR spectra of the products obtained at 20, 16, and 12 h of reaction time correspond to a mixture of compounds in which the unknown phase appears. The IR spectrum of this unknown product obtained after 4 and 8 h of reaction time (Figure 1b) shows the absence of any absorption band in the 3000−2600 cm^{-1} region and at ca. 1585 cm^{-1}. Furthermore, the spectrum shows absorption bands in the 1150−990 and 590−465 cm^{-1} regions, in good agreement with the existence of the P−O bonds. A weak band at a frequency of ca. 2460 cm^{-1} (2475 cm^{-1} with medium intensity in the Raman spectrum) indicates the presence of the H−P bond of the phosphite group. These results allow us to propose that a manganese(II) phosphite exists in the reaction medium, after 4 and 8 h of hydrothermal reaction, as the main phase. It disappears as a solid compound after ca. 24 h of reaction, giving rise to $(C_2H_{10}N_2)[Mn_3(HPO_3)_4]$, as can be observed from the X-ray powder diffraction patterns.

Crystal Structure. The structure of $(C_2H_{10}N_2)[Mn(HPO_3)_4]$ consists of anionic sheets of formula $[Mn_3(HPO_3)_4]^{2-}$, stacked along the [001] direction, whose charge is compensated by the ethylenediammonium cations displayed between the layers (Figure 2a). The sheets are constructed from manganese(II) cations with octahedral environment, giving rise to trimeric entities in which the octahedra are sharing faces. The phosphorus(III) ions from the $(HPO_3)^{2-}$ phosphite anions are four-coordinated, with a vertex of the tetrahedron occupied by the hydrogen atom and the oxygen atoms being coordinated to the Mn(II) ions. The HPO_3 tetrahedra link the trimeric units which are extended along the *ab* plane (Figure 2b).

It is worth mentioning the presence of the Mn_3O_{12} trimer clusters stacked along the *c* axis, which are formed from MnO_6 face-sharing octahedra (Figure 2c). In the $Mn(1)O_6$ octahedra the Mn(1) ion is bonded to the O(1), $O(1)^i$, O(4), $O(4)^i$, and O(6), $O(6)^i$ oxygen atoms, belonging to the $HP(2)O_3$ tetrahedra, with similar bond distances of 2.216(2) Å (×2), 2.214(1) Å (×2) and 2.215(1) Å (×2), respectively. The *cis*-O−Mn(1)−O angles range from 81.83(6)° to 98.17(6)°. The *trans*-O−Mn(1)−O angles are practically 180°, due to the special position occupied by the Mn(1) ions. The distortion of this polyhedron, from an octahedron ($\Delta = 0$) to a trigonal prism ($\Delta = 1$), calculated by quantification of the Muetterties and Guggenberger description,[35,36] is $\Delta = 0.11$, which indicates a topology near octahedral. In the $Mn(2)O_6$ octahedra the Mn(2) ion is bonded to the O(2), $O(5)^{iii}$ and O(1), O(4) oxygen atoms, belonging to the $HP(1)O_3$ and $HP(2)O_3$ tetrahedra, respectively, with bond distances of 2.110(2), 2.108(2) Å and 2.278(1), 2.285(2) Å, respectively. The longer distances correspond to the bonds established with the O(1) and O(4) oxygen atoms which are shared between the $Mn(1)O_6$ and $Mn(2)O_6$ octahedra. The other two positions of the $Mn(2)O_6$ octahedra are occupied by the $O(3)^{ii}$ and O(6) atoms, belonging to the $HP(1)O_3$ and $HP(2)O_3$ tetrahedra, respectively, with a short bond distance of 2.111(2) Å and a longer distance of 2.288(2) Å, respectively. The *cis*-O−Mn(2)−O angles range from 78.85(6)° to 98.30(5)°. The *trans*-O−Mn(2)−O angles deviate from the ideal value by approximately 8°. The distortion of this polyhedron, from an octahedron ($\Delta = 0$) to a trigonal prism ($\Delta = 1$), is $\Delta = 0.10$, which also indicates a topology near octahedral.

The HPO_3 tetrahedra exhibit similar P−O bond distances, with a mean value of 1.529(3) Å. The H(1)−P(1) and H(2)−P(2) bond distances are practically similar in both phosphite anions. The O−P−O angles are in the range from 110.8(1)° to 113.4(1)°, while the H−P−O angles range from 104(1)° to 109(1)°. In the ethylenediammonium cation, the C−C and C−N bond distances are in the range usually found for this molecule[37] and the angles are practically similar to those expected for a sp^3 hybridation. The ethylenediammonium cation is bonded by hydrogen bonds with the oxygen atoms of the $HP(1)O_3$ anion, linking the $[Mn_3(HPO_3)_4]^{2-}$ inorganic sheets of the compound. The bond lengths and angles are H(3)···$O(2)^i$−P(1), 1.904(1) Å, 106.86(9)°; H(4)···$O(3)^{ii}$−P(1), 1.919(2) Å, 107.8(1)°, and H(5)···$O(5)^i$−P(1), 1.890(2) Å, 105.55(7)° [i = $x, y + 1, z$; ii = $x, y - 1, z$].

(35) Muetterties, E. L.; Guggenberger, L. J. *J. Am. Chem. Soc.* **1974**, *96*, 1748.
(36) Cortes, R.; Arriortua, M. I.; Rojo, T.; Solans, X.; Beltran, D. *Polyhedron* **1986**, *5*, 1987.
(37) Gharbi, A.; Jouini, A.; Averbuch-Pouchot, M. T.; Durif, A. *J. Solid State Chem.* **1994**, *111*, 330.

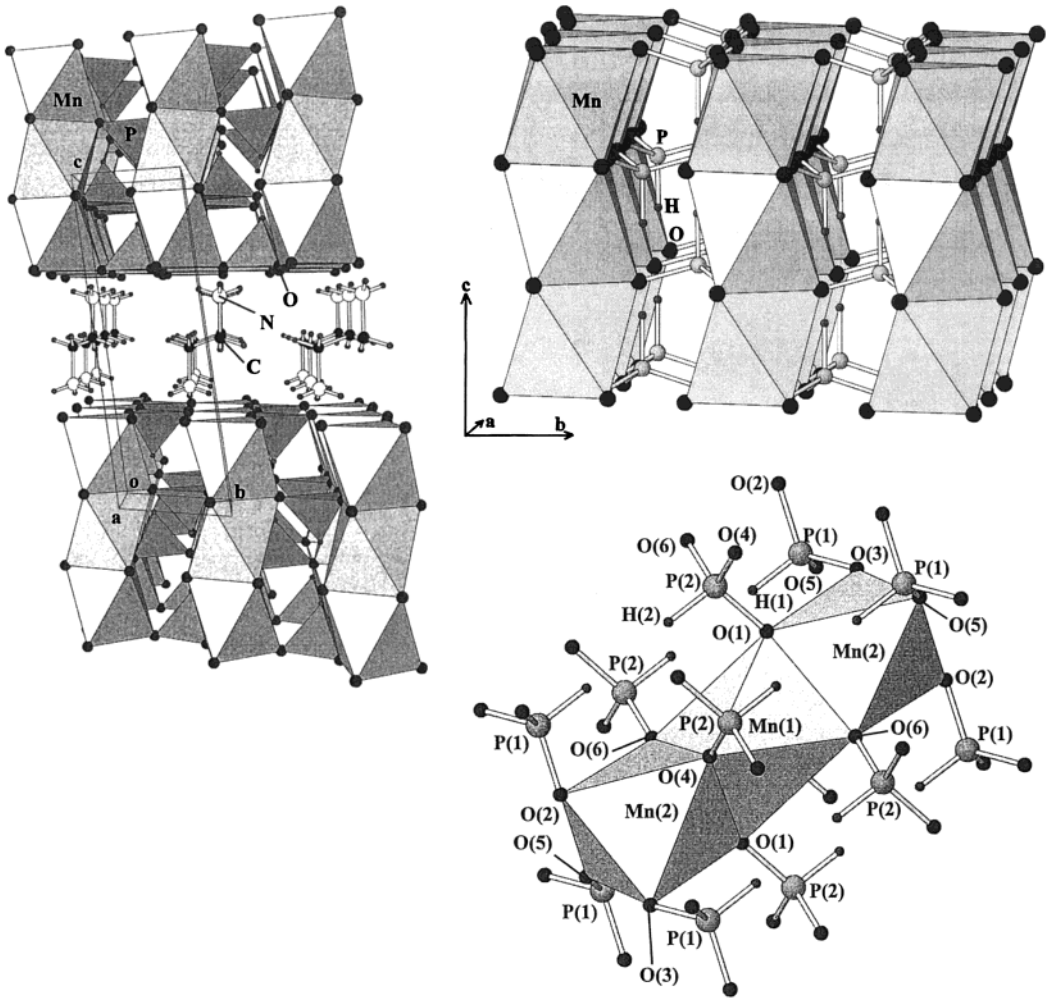

Figure 2. (a, left) Polyhedral view of $(C_2H_{10}N_2)[Mn_3(HPO_3)_4]$, showing the layered structure. (b, right top) Polyhedral representation of the $[Mn_3(HPO_3)_4]^{2-}$ sheets. (c, right bottom) View of the Mn_3O_{12} cluster of $(C_2H_{10}N_2)[Mn_3(HPO_3)_4]$ with detailed labeling of the atoms.

Infrared and Raman Spectroscopies. The infrared and Raman spectra of $(C_2H_{10}N_2)[Mn_3(HPO_3)_4]$ show the bands corresponding to the vibrations of the ethylenediammonium cation and phosphite $(HPO_3)^{2-}$ anions. The stretching mode of the $(NH_3)^+$ group, in the ethylenediammonium cation, appears at approximately 3165 cm^{-1} as a weak band. The band near 1585 cm^{-1} can be assigned to the $(NH_3)^+$ bending vibration. This band is indicative of the presence of the ethylenediamine molecule in its protonated form,[37,38] in good agreement with the structural results. The stretching vibrations of the $-CH_2-$ groups in the ethylenediammonium appear in the 3000−2600 cm^{-1} range, while the bending modes of these groups can be observed in the 1525−1465 cm^{-1} range. Different groups of bands can be attributed to the vibrational modes of the $(HPO_3)^{2-}$ anions present in the compound.[39,40] The stretching vibrations of the H−P groups in the phosphite anions are detected at similar frequencies, 2475 and 2435 cm^{-1}, in both IR and Raman spectra. The bending modes of this group appear at frequencies 1020, 995 cm^{-1} and 1025, 1010 cm^{-1} in the IR and Raman spectra, respectively. The asymmetric and symmetric stretching vibrations of the PO_3 groups can be observed at 1135, 1085 cm^{-1} and 980 cm^{-1}, respectively, in the IR spectrum, while in the Raman spectrum these modes appear at frequencies 1070, 1060 cm^{-1} and 990 cm^{-1}, respectively. Finally, the symmetric and asymmetric PO_3 deformation modes can also be observed in the spectra. The former appear at approximately 640, 620 cm^{-1} and 650, 600 cm^{-1} in the IR and Raman spectra, respectively. The asymmetric modes are detected at frequencies of 490 and 465 cm^{-1} in the IR spectrum and at 490 and 450 cm^{-1} in the Raman spectrum.

UV−Vis and Luminescence Spectroscopies. Luminescence measurements of the Mn(II) ion in $(C_2H_{10}N_2)[Mn_3(HPO_3)_4]$ have been carried out at 6.0 K. Figure 3a displays the emission spectrum of the compound obtained under a 365 nm excitation. It exhibits a unique red emission peaking at 651 nm which is characteristic of an octahedral environment for the Mn(II) (d^5) ions. The excitation spectrum ($\lambda_{em} = 680$ nm) (Figure 3b) reveals the spectral distribution of bands corresponding to the excited levels of Mn(II) [$^4T_1(^4G)$, 550 nm; $^4T_2(^4G)$, 447 nm; $^4A_1,^4E(^4G)$, 406 nm; $^4T_2(^4D)$, 366 nm; $^4E(^4D)$, 342 nm]. These values agree with those generally observed for Mn(II) in an octahedral site.[41,42] The diffuse reflectance spectrum of this compound

(38) Dolphin, D.; Wick, A. E. *Tabulation of infrared spectral data*; John Wiley & Sons: New York, 1977.
(39) Tsuboi, M. *J. Am. Chem. Soc.* **1957**, *79*, 1351.
(40) Nakamoto, K. *Infrared and Raman spectra of inorganic and coordination compounds*; John Wiley & Sons: New York, 1997.

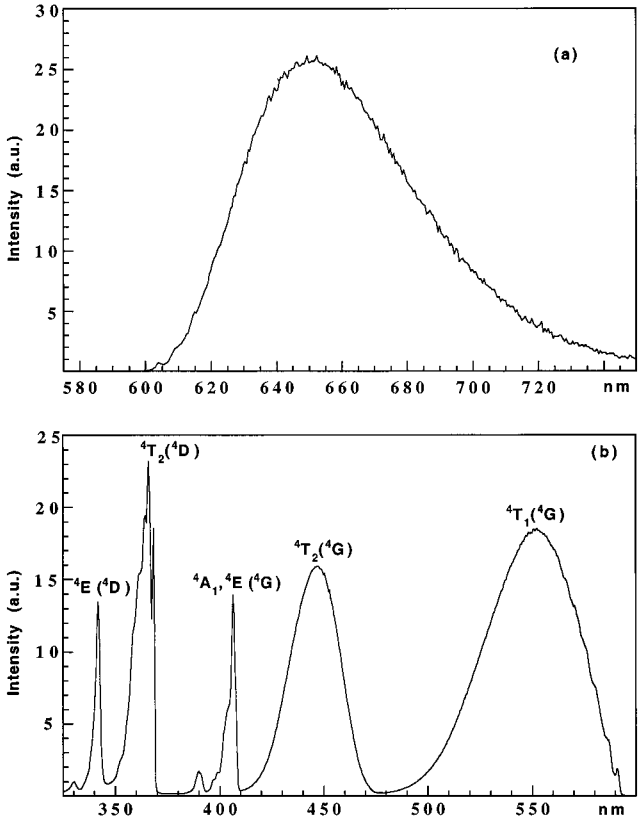

Figure 3. (a) Emission spectrum (λ_{exc} = 365 nm) and (b) excitation spectrum (λ_{em} = 680 nm) of $(C_2H_{10}N_2)[Mn_3(HPO_3)_4]$ at 6.0 K.

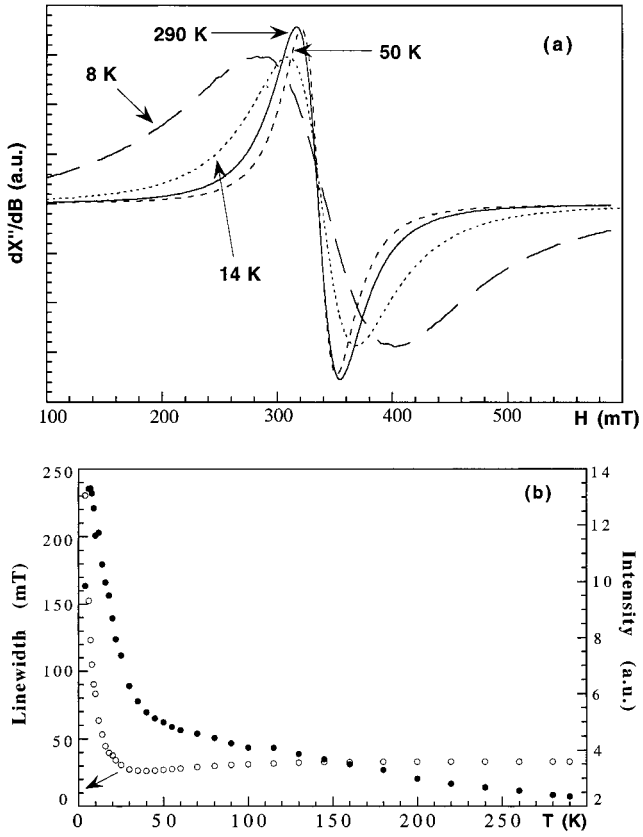

Figure 4. (a) Powder X-band ESR spectra of $(C_2H_{10}N_2)[Mn_3(HPO_3)_4]$, at different temperatures. (b) Temperature dependence of the intensity of the signal and the line width curves.

exhibits several very weak spin-forbidden d−d bands, at approximately 340, 365, 405, 440, and 540 nm. The position of these bands is similar to that obtained from the luminescence results and therefore can be assigned to the Mn(II) ions in an octahedral environment.

Taking into account the results of the luminescence and diffuse reflectance spectroscopies, the Dq and Racah parameters have been calculated by fitting the experimental frequencies to an energy level diagram for an octahedral d^5 high-spin system.[43] The values obtained are Dq = 875, B = 660, and C = 3610 cm^{-1}. These values are in the range usually found for octahedrally coordinated Mn(II) compounds.[24,44,45]

ESR and Magnetic Properties. ESR spectra of $(C_2H_{10}N_2)[Mn_3(HPO_3)_4]$ have been recorded on a powdered sample at the X-band between 4.2 and 300 K and are given in Figure 4a. The spectra remain essentially unchanged upon cooling the sample from 300 to 50 K. Below this temperature, however, the signal broadens and loses intensity. The spectra are isotropic with a "g" value of ca. 2.01, which remains unchanged with variation in temperature. This g value is characteristic of octahedrally coordinated Mn(II) ions. The temperature dependence of the intensity and the line width of the signals calculated by fitting the experimental spectra to Lorentzian curves are displayed in Figure 4b. The intensity of the signal increases in the temperature range studied, and does not exhibit any substantial decrease at low temperatures. The diminution observed below ca. 5 K is probably due to an effect of integration of the signal, caused by the long line width of the curve at this temperature. This behavior could be explained considering the compound as either a paramagnetic or an antiferromagnetic system in which the maximum in the magnetic susceptibility appears at temperatures lower than 4.2 K, the minimum temperature at which the ESR spectrometer used in the experiment operates. The line width of the ESR signal remains practically unchanged from room temperature to ca. 30 K. When the temperature is further decreased, the line width increases vigorously due to a strong spin correlation. These results are in good agreement with those observed for other magnetic systems, in which the line width also increases drastically when the temperature approximates the critical one.[46−50]

Variable-temperature magnetic susceptibility measurements of $(C_2H_{10}N_2)[Mn_3(HPO_3)_4]$ have been carried out on a powdered sample in the range from 4.2 to 300 K. The plots of the χ_m and $\chi_m T$ vs T curves are shown in Figure 5. The molar magnetic susceptibility increases

(41) Orgel, L. E. *J. Chem. Phys.* **1955**, *23*, 1004.
(42) Tanabe, Y.; Sugano, S. *J. Phys. Soc. Jpn.* **1954**, *9*, 753.
(43) Lever, A. B. P. *Inorganic electronic spectroscopy*; Elsevier Science Publishers B.V.; Amsterdam, The Netherlands, 1984.
(44) Lawson, K. E. *J. Chem. Phys.* **1966**, *44*, 4159.
(45) Escobal, J.; Mesa, J. L.; Pizarro, J. L.; Lezama, L.; Olazcuaga, R.; Rojo, T. *J. Mater. Chem.* **1999**, *9*, 2691.
(46) Wijn, H. W.; Walker, L. R.; Daris, J. L.; Guggenheim, H. *J. Solid Sate Commun.* **1972**, *11*, 803.
(47) Richards, P. M.; Salamon, M. B. *Phys. Rev. B* **1974**, *9*, 32.
(48) Escuer, A.; Vicente, R.; Goher, M. A. S.; Mautner, F. *Inorg. Chem.* **1995**, *34*, 5707.
(49) Bencini, A.; Gatteschi, D. *EPR of exchange coupled systems*; Springer-Verlag: Berlin, Heidelberg, 1990.
(50) Cheung, T. T. P.; Soos, Z. G.; Dietz, R. E.; Merrit, F. R. *Phys. Rev. B* **1978**, *17*, 1266.

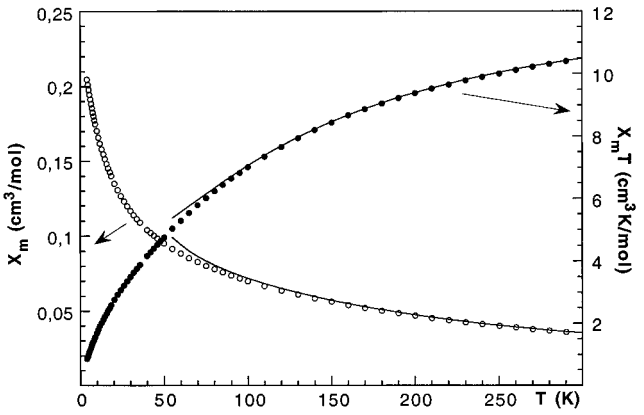

Figure 5. Thermal evolution of χ_m and $\chi_m T$ curves of $(C_2H_{10}N_2)[Mn_3(HPO_3)_4]$. The solid lines show the fit of the χ_m and $\chi_m T$ experimental data to a model for isolated trimers.

with decreasing temperature in the range studied. The $\chi_m T$ product decreases from 10.48 cm^3 K/mol at 300 K to 0.87 cm^3 K/mol at 4.2 K. The room-temperature $\chi_m T$ value, 10.48 cm^3 K/mol, is smaller than the expected value, 13.26 cm^3 K/mol, for three Mn(II) ions uncoupled with $S_i = 5/2$ and $g_i = 2.01$. This result is indicative of substantial antiferromagnetic coupling, which is confirmed by the dramatic decrease of $\chi_m T$ when T decreases.

Considering the structural features of this compound, in which the $[Mn_3(HPO_3)_4]^{2-}$ inorganic sheets are formed by linear trimeric units of Mn(II) ions extended along the *c* axis, we have analyzed the magnetic data by using the Heisenberg Hamiltonian for a trimeric system

$$H_S = -J(S_1 \cdot S_2 + S_2 \cdot S_3) - J_{13} S_1 \cdot S_3$$

where S_i is the spin of the Mn ion number *i* in Figure 2c. The Van Vleck expression for the susceptibility is

$$\chi = [Ng^2\beta^2/3kT][u/u'] \qquad (1)$$

with $u = \sum_{S_{13},S} S(S+1)(2S+1)\exp(-E(S_{13},S)/kT)$ and $u' = \sum_{S_{13},S}(2S+1)\exp(-E(S_{13},S)/kT)$. The value of the $E(S_{13},S)$ energy levels has been taken from ref 51, considering a linear trimer where $J_{13} = 0$. The results obtained in the fit are shown in Figure 5. It can be observed that only the magnetic data above ca. 80 K can be fitted to eq 1 with a value of the J exchange parameter of −17 K and $g = 2.0$ (solid lines in Figure 4). Considering the existence of magnetic interactions between neighboring trimers connected via phosphite anions, a J' exchange parameter was introduced in eq 1, but the fit did not show a substantial improvement. A possible explanation of these results should consider that at high temperatures the compound can be described as a linear isolated trimer, but at low temperatures strong intertrimer interactions propagated via phosphite anions along the sheets are predominant in the compound. This explanation is supported by the $\chi_m T$ curve, which at low temperature shows a value for $\chi_m T$ of 0.87 cm^3 K/mol instead of the expected value of 4.37 cm^3 K/mol for an uncoupled Mn(II) ion with spin $S = 5/2$ and $g =$ ca. 2.0. On the basis of this assumption we have tried to analyze the low-temperature magnetic data by considering the compound as a two-dimensional system of spin $S = 5/2$, but the known 2D magnetic model does not give rise to good results. Therefore, we could conclude that at low temperatures the compound shows a complex magnetic behavior as the result of a long magnetic order established at temperatures lower than ca. 80 K.

(51) Kahn, O. *Molecular magnetism;* VCH Publishers: New York, 1993.

Concluding Remarks

The compound with formula $(C_2H_{10}N_2)[Mn_3(HPO_3)_4]$ has been synthesized under hydrothermal conditions. This is the first inorganic−organic hybrid manganese(II) phosphite. The evolution of the reaction mixture as a function of the reaction time has been studied, and the intermediates obtained have been characterized by X-ray powder diffraction and IR and Raman spectroscopies. The results indicate that the compound is formed after the mixture is heated for ca. 24 h under vapor pressure of water at a temperature of 170 °C. However, the synthesis of suitable single crystals for the X-ray diffraction study needs a reaction time of at least ca. 5 days. The IR and Raman spectroscopies reveal the existence of a manganese(II) phosphite in the first steps of the hydrothermal synthesis. This result shows that preferentially an insoluble inorganic phosphite is formed in the process of the synthesis of an inorganic−organic hybrid compound, against other possible intermediates. The crystal structure of $(C_2H_{10}N_2)[Mn_3(HPO_3)_4]$ consists of inorganic sheets of composition $[Mn_3(HPO_3)_4]^{2-}$, with ethylenediammonium cations located in the interlayer region. Within the sheets, the Mn(II) ions exhibit an octahedral environment. These polyhedra show face-sharing, giving rise to trimer units linked by $(HPO_3)^{2-}$ tetrahedra anions. From the luminescence and reflectance diffuse measurements the Dq and Racah (*B* and *C*) parameters have been calculated. The values are in the range usually found for Mn(II) ions in octahedral sites. The ESR spectra are isotropic with a *g* value of 2.01, which remains unchanged from room temperature to 4.2 K. The intensity and the line width of the ESR signals increase in the range 300−4.2 K. Magnetic measurements up to 4.2 K indicate the presence of antiferromagnetic interactions. The magnetic data above ca. 80 K have been fitted to a model for linear isolated trimers with a J value of −17 K. At low temperatures the compound does not behave as a simple isolated trimer, and probably a long magnetic order is established due to the strong intertrimer interactions, which are propagated along the sheets via phosphite anions.

Acknowledgment. This work was financially supported by the Ministerio de Educación y Ciencia and Universidad del País Vasco/EHU (Grants PB97-0640 and 169.310-EB149/98, respectively), which we gratefully acknowledge. We thank F. Guillen (ICMCB, Pessac, France) for luminescence measurements at low temperature. S.F. thanks the Gobierno Vasco/Eusko Jaurlaritza for a doctoral fellowship.

Supporting Information Available: Crystallographic data and structure factors for $(C_2H_{10}N_2)[Mn_3(HPO_3)_4]$. This material is available free of charge via the Internet at http://pubs.acs.org.

CM001026S